Modeling and Development of RMD Configuration Magnetic Bearing

K.P. Lijesh[a], H. Hirani[a]

[a] Indian Institute of Technology, Delhi, New Delhi, India.

A B S T R A C T

The low load carrying capacity of Passive Magnetic Bearings (PMBs) has restricted their use in many industrial applications. The Rotation Magnetized Direction (RMD) configuration has emerged as a strong and viable method that is able to substantially enhance the load carrying capacity of passive magnetic bearings. It consists of both radially and axially polarized passive magnets. But the physical realization of a radially polarized magnet is difficult to achieve. In the present work, a RMD structure consisting of aluminum ring and cubical shaped magnets is proposed by developing the radially polarized magnets required for RMD structure.

A theoretical model is derived by simulating the cuboid magnets in form of sector magnets by developing equivalent surface area. An experimental setup was designed and developed to conduct experimental verification. The theoretical model is validated by conducting experiments on RMD configuration magnetic bearing and axially magnetized full ring bearing. The comparison of the load carrying capacity by different configuration is performed and results are presented.

1. INTRODUCTION

Bearings are broadly classified into (i) ball bearing [1-2], (ii) journal bearing [3-6] and magnetic bearing [7-9]. In the present work Passive Magnetic Bearings (PMB) is considered. PMB's are known for the non-contact and friction less characteristics and thus finds extensive usage in several applications like high speed compressors [10], flywheel energy storage systems [11-12] etc. However, its low load carrying capacity has restricted its use in common applications. The Halbach arrangement [13-16] is generally employed to overcome this drawback by increasing its load capacity. In the present research work, one of the Halbach arrangements, namely, Rotation Magnetized Direction (RMD) configuration is used. The RMD configuration is achieved by stacking of both radial and axial polarized magnets as shown in Fig. 1.

One major drawback of RMD configuration is that physical realization of radially magnetized full ring magnets [15-16] is very difficult to achieve. Since a cubical shape magnet (magnetized through its thickness), if appropriately assembled, can be used to generate axial as well as a radial polarized

magnets. Therefore, in the present research work a structure has been proposed that consists of cubical slots for incorporating cubical magnets to achieve radial magnetization. The theoretical and experimental load carrying capacity of the magnetic bearing with full ring axial polarized magnet and RMD configuration is carried out and results are presented.
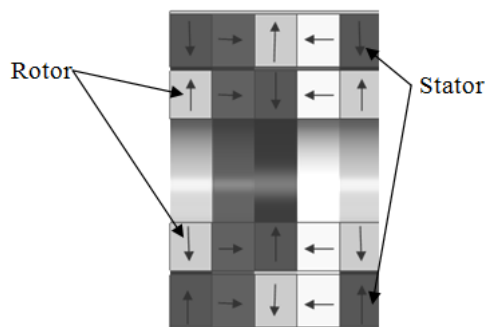
Fig. 1. RMD configuration.

Fig. 1. RMD configuration.
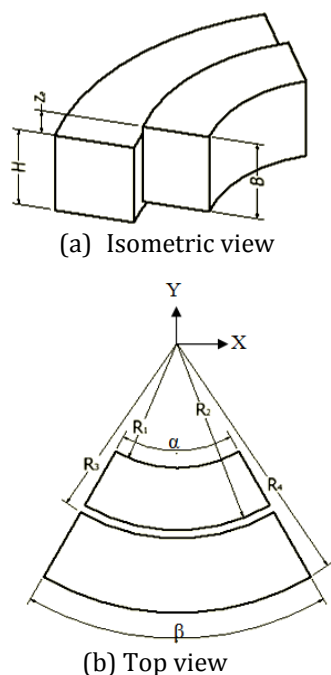

(a) Isometric view

(b) Top view

Fig. 2. Sector magnets.

A novel method for the determination of the theoretical load carrying capacity of a cuboid magnet is proposed wherein the load carrying capacity of a sector magnet and cuboid magnet are equalized by equating their surface area and volume. This task is challenging because of the absence of the curvature in the cuboid magnet and consequent non-applicability of cylindrical coordinate system. Based on these considerations, the theoretical load carrying capacity of different arrangements is then estimated using 3D Coulombian model [17-21].

The comparison of the load carrying capacity of two sector magnets (Fig. 2) and two cuboid magnets (Fig. 3) having the same surface area and volume (since the force generated by a magnets is contributed by the charge distributed on the surfaces of the magnet) is performed.
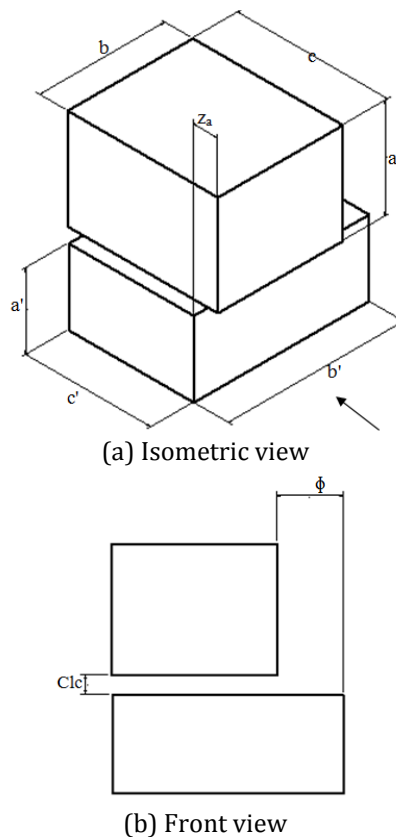

(a) Isometric view

(b) Front view

Fig. 3. Cuboidal magnets.

The validation of the proposed method is carried out by developing an experimental setup for the measurement of the static load carrying capacity and conducting experiments at different eccentricities for full ring and RMD configuration bearings.

2. MATHEMATICAL MODELING AND VALIDATION

In permanent magnetic bearing (PMB) rotor magnet is assembled on shaft and stator magnet is fixed in the housing. Due to repulsion between stator and rotor magnets, shaft remains in levitate position even under loaded conditions. Using 3D Coulombian model [21] the vertical force is estimated for the following configurations: (i) Configuration 1: Axially polarized full ring rotor and stator magnets (Fig. 4) and (ii) Configuration 2: RMD configuration (Fig. 5).

$$R(\alpha) = \int_{\theta_3}^{\theta_4} \int_{\theta_1}^{\theta_2} \int_{R_3}^{R_4} \int_{R_1}^{R_2} \left[\frac{\left(e + r_{12}\cos(\theta) - r_{34}\cos(\theta')\right) r_{12} r_{34}}{\left(r_{12}^2 + r_{34}^2 + e^2 - 2r_{12}r_{34}\cos(\theta - \theta') + 2e\left(r_{12}\cos(\theta) - r_{34}\cos(\theta')\right) + (\alpha)^2\right)^{1.5}} \, dr_{12} dr_{34} d\theta d\theta' \right] \quad (2)$$
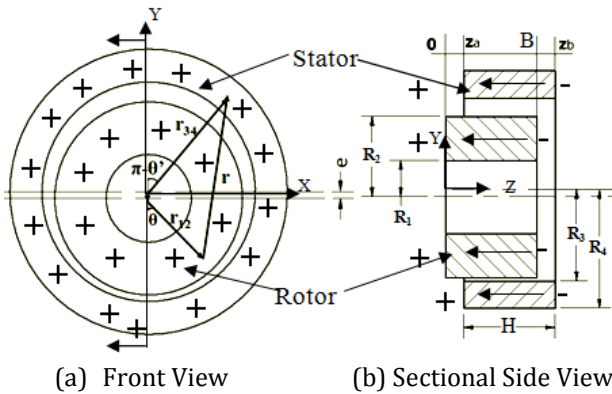

(a) Front View   (b) Sectional Side View

Fig. 4. Configuration 1: coordinates of Magnetic bearing.
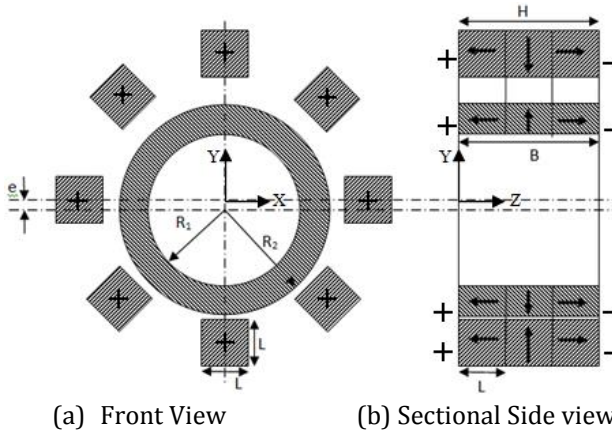

(a) Front View   (b) Sectional Side view

Fig. 5. Configuration 2: RMD configuration.

According to Coulombian model, axially polarized magnet is represented by two charged planes located on the front and back side as shown in Figs. 4(a) and 5(a) or left and right side surfaces of the magnet, as shown in Figs. 4(b) and 5(b). '+' sign denotes the one of the plane (north-pole) and '-' sign shows the other plane (south pole). The charge distribution in the front plane of ring permanent magnet is $+\sigma$ and in the back side is $-\sigma$. σ_1, σ_2 are the charge distributions of the stator and rotor magnets respectively. In the following sections discussion on the vertical force estimation of different configuration is carried out.

### 2.1 Mathematical Modelling for Configuration 1

The vertical force exerted by two axially polarized full ring magnets can be estimated by Colombian model provided by Tan et al. [18] and

Hirani and Samanta [19] and is represented in equation (1).

$$F_y = \frac{\sigma_1 \sigma_2}{4\pi\mu_0} \left(R(z_a) + R(z_a + H - B) + R(z_a + H) + R(z_a - B) \right) (1)$$

Where $R(\alpha)$ is given by (2).

Where 'e' is the eccentricity between the rotor and stator magnet, 'R_1' and 'R_2' is the inner and outer radius of the rotor magnet and 'R_3' and 'R_4' is inner and outer radius of the stator magnet as shown in Fig. 4(a). H and B are the axial length of the stator and rotor magnets respectively. z_a is the axial offset between the rotor and stator magnet as shown in Fig. 4(b). The value of 'θ' varies from '$\theta_1=0$' and '$\theta_2=2\pi$' for full ring rotor and value of 'θ'' varies from '$\theta_3=0$' and '$\theta_4=2\pi$' for a full ring stator magnet.
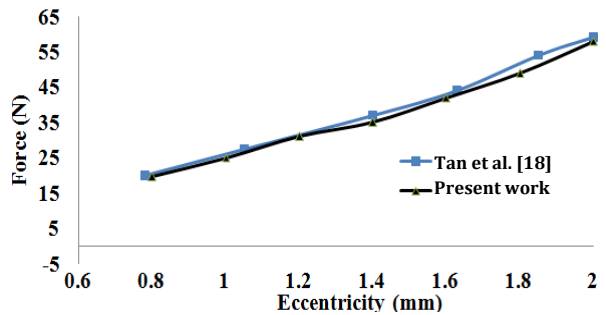
(a) Tan et al. [18]
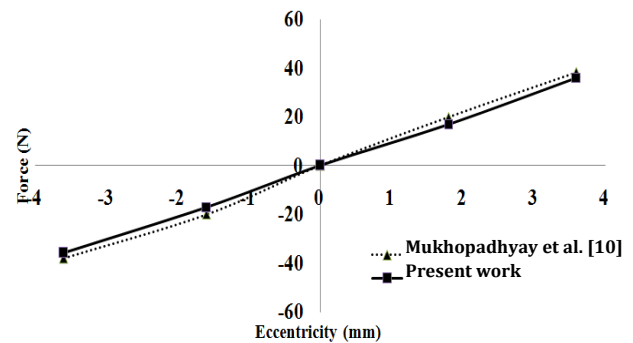
(b) Mukhopadhyay et al. [10]

Fig. 6. Load comparison of present work with Tan et al. [18] and Mukhopadhyay et al. [10].

It can be observed that equation (1) have four integrations and in the present work these four integrations have been solved using trapezoidal numerical integration technique in MATLAB software. The validation of the program has been carried out by comparing the solution

obtained from the MATLAB coding and established literatures [12,18] and the results are plotted in Fig. 6. From this figure it can be concluded that the developed code is correct and can be extended for the present work.

2.2 Mathematical Modelling for Configuration 2

For developing theoretical formulation for RMD configuration (Fig. 5), the load carried by the repulsion force between two radially polarised magnets (Fig. 7(a)) and perpendicular polarized magnets (Fig. 7(b)) are to be formulated. The total load carrying capacity of RMD configuration ($F_{y,RMD}$) is given by:

$$F_{y,RMD}= \Sigma[\Sigma(\text{Radial polarized})+\Sigma(\text{Axial polarized})+\Sigma(\text{Perpendicular polarized})] \quad (3)$$
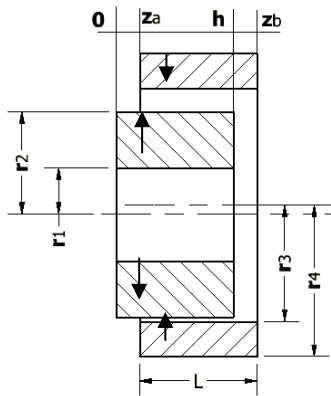
(a) Radially polarized magnetic bearing
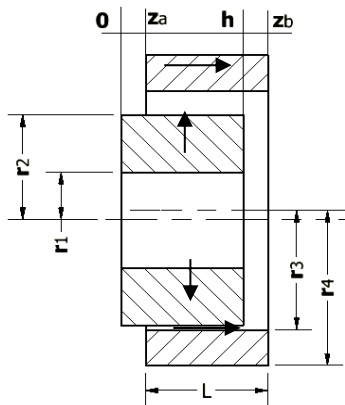
(b) perpendicular polarized magnetic bearings

Fig. 7. the radial and perpendicular polarized magnetic bearings.

Yonnet [15] proved that for an identical bearing, the load carrying capacity between two radial polarized magnets remains same as load capacity between two axial polarized magnets. Hence a separate formulation for radial polarized magnets is not required and the equation (3) can be modified for the present case as:

$$F_{y,RMD}=\Sigma[3x(\text{Axial polarized})+ 4 \; x \; (\text{Perpendicular polarized})] \quad (4)$$

A separate modelling for perpendicularly polarized magnets is required, formulation of which is described in the following section.

Mathematical Modelling for Perpendicularly Polarized Magnets

In perpendicularly polarized magnetic bearing, the polarization direction between rotor and stator is perpendicular to each other. For example in Fig. 7(b) the rotor is radially polarized and stator is axially polarized. The vertical force between the two rings in a perpendicularly polarized magnetic bearing ($F_{y,p}$) is represented as:

$$F_{y,p}=A(z_a,R_1)-A(z_a+h,R_1)-A(z_a,R_2)+A(z_a+h,R_2) \quad (5)$$

where $A(z_a,R_1)$, equation (6).

Total load carrying of the RMD configuration

For a full ring RMD configuration there can be seven different possible arrangements as shown in Fig. 11. In 'arrangement 1' the force is exerted between two axially polarized magnets and the force exerted between the magnets can be estimated using equation (1). Similarly 'arrangement 2', consists of a axial polarized stator and radial polarized rotor magnets, which are in perpendicular polarization to each other hence the force exerted for this arrangement can be estimated using equation (5).

In 'arrangement 3' the force is exerted between two radial polarized magnets which can be estimated using equation (1). Same way the load carrying capacity of other arrangements can be calculated and summed to find the total load carrying capacity.

$$A\left(z_a,R_1\right)=\int_0^{2\pi}\int_0^{2\pi}\int_0^L\int_{R_3}^{R_4}\frac{\left(e+R_1\cos(\theta)-r_{34}\cos(\theta')\right)}{\left(R_1{}^2+r_{34}{}^2+e^2-2R_1r_{34}\cos(\theta-\theta')+2e\left(R_1\cos(\theta)-r_{34}\cos(\theta')\right)+(z_a-z_{34})^2\right)}dr_{34}dz_{ab}d\theta d\theta' \quad (6)$$

The total vertical force for RMD configuration ($F_{y,RMD}$) is estimated by summing the individual force by the magnets in axial and perpendicular polarization. The total vertical force by RMD configuration is given by equation (12).

$$F_{y,RMD} = \sum \left(\sum_{j=1}^{k} F_{y,s,i,j} + \sum_{j=1}^{m} F_{y,p,i,j} \right) \quad (7)$$

Where 'k' is the number of segments of radial and axial polarized magnets and 'm' is number of perpendicular polarized magnet in RMD configuration. For example in the present case as shown in Fig. 11, there are three (two axial + one radial) axially polarized magnets and four perpendicular polarized magnets, the modified equation (7) is given in equation (8):

$$F_{y,RMD} = \sum \left(3 \times \sum_{i=1}^{n} F_{y,s,i,j} + 4 \times \sum_{i=1}^{n} F_{y,p,i,j} \right) \quad (8)$$
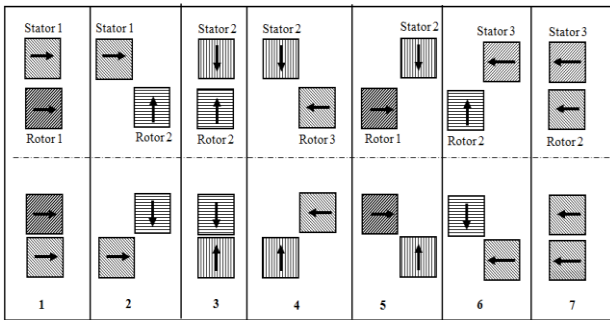

Fig. 11. Different arrangements of RMD configurations.

## Mathematical modelling of RMD configuration with cubical magnets

The realization of the radial polarized magnets are difficult and also unavailability of the magnets of desired size, in the present work a stator of the magnetic bearing is developed which consists of a aluminum structure with cubical slots as shown in Fig. 12(a) is developed. Similarly a structure is made for rotor for achieving the radially polarization as shown in Fig. 12(b) and cubical magnets are inserted in the slots.

The bearing developed in the present work consists of number of cubical magnets both in stator and rotor and representing cubical magnets in the cylindrical coordinates is a incorrect approach. An attempt was made to replace the cubical magnet with sector magnets having equivalent surface area, since representing sector magnets in cylindrical coordinates is easier. In the present work using

3D Coulombian model, the load between two cuboid (cubical is a sub class of cuboid when the sides of cuboid are equal) magnets on a ring magnet or between two cuboid magnets is estimated by replacing a cuboid magnets with a sector magnets.
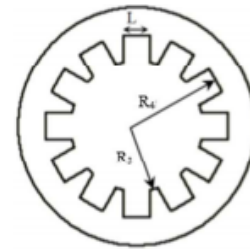
(a) Stator Structure.
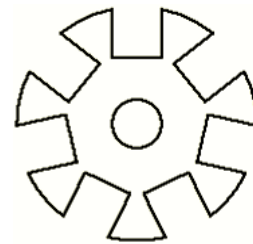
(b) Rotor structure for radial polarization.

Fig. 12. Stator and Rotor structure for RMD configuration.

As per the Coulombian model the charges of magnets are distributed on the surfaces of the magnet and in turn contribute for the strength of the magnet. Hence it was hypothesised that the magnets having same surface areas have same load carrying capacity and to validate this hypothesis the load carrying capacity between two sector magnets and cubical magnets having same surface area was compared. In the following paragraphs the Coulombian model for sector and cuboid magnet is shown and results were compared.

3D Coulombian model for the force between two sector magnets in vertical (Y) direction ($F_{y,s}$) (Fig. 2) can be derived from equation (1) by replacing the value of 'θ_1' by $-\alpha/2$, 'θ_2' by $\alpha/2$, 'θ_3' by $-\beta/2$ and 'θ_4' by $\beta/2$. The modified vertical force equation (1) for a sector magnet ($F_{y,s}$) is given in equation (9).

$$F_{y,s} = \frac{\sigma_1 \sigma_2}{4\pi\mu_0} \left(R(z_a) + R(z_a + H - B) + R(z_a + H) + R(z_a - B) \right) \quad (9)$$

where:

$$R(\alpha) = \int_{-\frac{\alpha}{2}}^{\frac{\alpha}{2}} \int_{-\frac{\beta}{2}}^{\frac{\beta}{2}} \int_{R_3}^{R_4} \int_{R_1}^{R_2} \frac{\left(e + r_{12}\cos(\theta) - r_{34}\cos(\theta') \right) r_{12} r_{34}}{\left(\begin{array}{c} r_{12}^2 + r_{34}^2 + e^2 - 2r_{12}r_{34}\cos(\theta - \theta') \\ +2e\left(r_{12}\cos(\theta) - r_{34}\cos(\theta') \right) + (\alpha)^2 \end{array} \right)^{1.5}} dr_{12} dr_{34} d\theta d\theta'$$

The load carrying capacity in vertical (Y) direction ($F_{y,c}$) between two cubical magnets (Fig. 3) is estimated using Colombian model provided by Akoun and Yonnet [21] and is represented in equation (10).

$$F_{y,c} = \frac{\sigma_1 \sigma_2}{4\pi\mu_0} \left(R(z_a) + R(z_a + b' - b) + R(z_a + b') + R(z_a - b) \right) \quad (10)$$

where:

$$R(\alpha) = \int_0^b \int_0^a \int_0^{b'} \int_0^{a'} \frac{(\gamma + Y - y)}{\left(\begin{array}{l} (\varphi + X - x)^2 + \\ (Clc + Y - y)^2 + (z_a + Z - z)^2 \end{array} \right)^{1.5}} dX dY dx dy$$

Designing sector magnets equivalent to cubical magnets or vice versa for same load carrying capacity, the thickness and axial length of sector and cubical magnets were assumed equal i.e. ($R_2 - R_1$)=a, ($R_4 - R_3$)=a', B=c and H=c' (from figures 2 and 3). The angular length of the both sector magnets are kept equal ($\alpha = \beta = \psi$) and estimated by equation suggested by Yonnet et al. [22] and given in equation (11):

$$\psi = \frac{2L}{(R_3 + R_2)} \quad (11)$$

The modified equation (8) is represented in equation (12):

$$R(\alpha) = \int_{-\frac{\Psi}{2}}^{\frac{\Psi}{2}} \int_{-\frac{\Psi}{2}}^{\frac{\Psi}{2}} \int_{R_3}^{R_4} \int_{R_1}^{R_2} \frac{(e + r_{12}\cos(\theta) - r_{34}\cos(\theta')) r_{12} r_{34}}{\left(\begin{array}{l} r_{12}^2 + r_{34}^2 + e^2 - 2r_{12}r_{34}\cos(\theta - \theta') + \\ 2e(r_{12}\cos(\theta) - r_{34}\cos(\theta')) + (\alpha)^2 \end{array} \right)^{1.5}} dr_{12} dr_{34} d\theta d\theta'$$

$$(12)$$

To validate the developed code for equations (9) and (10) in MATLAB, few examples for sector and cuboid magnet were considered from the established literatures [12,17,19,21] and results were compared. To validate the MATLAB code for equation (9), vertical load of magnetic bearing having full rotor magnet and different configurations of stators [12,17,19] has been considered. The dimensions considered for the validation has been obtained from [12,17,19] and are tabulated in Table 1.

Table 1. Dimensions of magnets considered for validation.

Sl. No.	Parameter	Mukhopadhyay et al. [12]	Muzakkir et al. [17]	Hirani et al. [19]
1	Inner radius of rotor (R_1) (mm)	20	0.05	10
2	Outer radius of rotor (R_2) (mm)	40	0.024	16
3	Inner radius of stator (R_3) (mm)	45	0.025	16.05

4	Outer radius of stator (R_4) (mm)	55	0.05	22
5	Axial length of rotor (B) (mm)	40	32	15
6	Axial length of stator (H) (mm)	50	30	15
7	Magnetic Remanance value of rotor (T)	1.17	0.8	1
8	Magnetic Remanance value of stator (T)	0.38	1	1

The comparison of the vertical forces obtained for different configuration by Hirani et al. [19] and present work has been tabulated in Table 2.

Table 2. Load carrying capacity comparison of present work with Hirani et al. [19].

Angle of Bottom angle magnet	Hirani et al. [9] (N)	Present work (N)
240°	59.7	59.6
180°	67.3	67.12
120°	57.8	57.5
60°	34	33.93

Vertical load values of 180° sector stator magnet for different eccentricity obtained from equation (9) is compared with Muzakkir et al. [17] and the results has been presented in the Table 3.

Table 3. Load carrying capacity comparison of present work with Muzakkir et al. [17].

Eccentricity (mm)	Muzakkir et al. [8] (N)	Present work (N)
0.2	353	352.5
0.4	358	357.1
0.6	365	364.8
0.8	370	368.5
0.99	378	377.3

Similarly comparison of the results form equation (9) and the results from Mukhopadhyay [12] has been represented in Fig. 12.
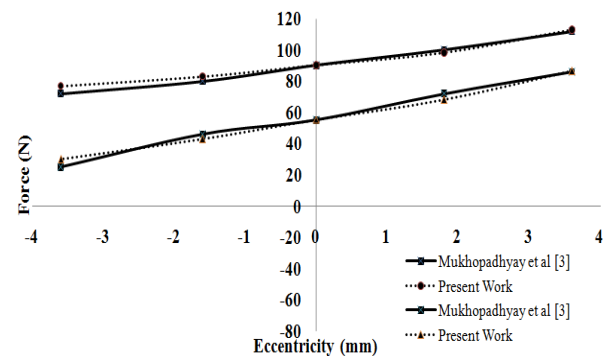

Fig. 12. Load carrying capacity comparison of present work with Mukhopadhyay et al. [12].

The dimensions for the cuboid magnets provided by [21] have been considered for the verification of the developed MATLAB code for equation (9). The results of vertical force exerted by two cuboid magnets [21] having flowing dimension: a=20 mm, b=12 mm, c=6 mm, A=12 mm, B=20 mm, C=6 mm, φ=-4 mm, ϕ=-4 mm, γ=8 mm was 0.6 N while the value of $F_{y,c}$ obtained from equation (5) was 0.63 N. The obtained result validates the MATLAB code generated for equation (10).

After gaining confidence on the developed MATALB code, the code was extended for the comparing the load-carrying capacity between two sector magnets and cubical magnet considering two case studies.

Case study 1: Consider two cubical magnets of sides L=20 mm and the distance between the magnets be 1 mm, calculate the load carrying capacity between the magnet and also calculate estimate the load carrying capacity of the equivalent sector magnets. Consider the magnetic remanence value of both the magnets as 1 T.

Solution: Here; (R_2-R_1)=L=(R_4-R_3)=L=B=c= H=c'=20 mm and Clc=1 mm. Assuming R_1=5 mm, R_2= 25 mm, R_3=26 mm and R_4=46 mm. The value of ψ is estimated from equation (11) i.e.

$$\psi = \frac{2L}{(R_3 + R_2)} = 0.783$$

The vertical force between two cubical magnets is found by using equation (10).

$$F_{y,c} = \frac{\sigma_1 \sigma_2}{4\pi\mu_0}\left(R(0) + R(0.02 - 0.02) + R(0.02) + R(-0.02)\right)$$

where:

$$R(\alpha) = \int_{0.021}^{0.041}\int_{0}^{0.02}\int_{0}^{0.02}\int_{0}^{0.02} \frac{(Y - y)}{\left((X-x)^2 + (Y-y)^2 + (\alpha)^2\right)^{1.5}} dXdYdxdy$$

The value of $F_{y,c}$ is estimated by solving the above equation in MATLAB and found to be 38.38 N.

The load carrying capacity of the equivalent sector magnet is found using equations (12). The modified equation after substituting the values z_a, B and H is as follows:

$$F_{y,s} = \frac{\sigma_1 \sigma_2}{4\pi\mu_0}\left(R(0) + R(0.02 - 0.02) + R(0.02) + R(-0.02)\right)$$

where:

$$R(\alpha) = \int_{-0.261}^{0.261}\int_{-0.261}^{0.261}\int_{0.026}^{0.046}\int_{0.005}^{0.025} \left[\frac{(r_{12}\cos(\theta) - r_{34}\cos(\theta'))r_{12}r_{34}}{\left[r_{12}^2 + r_{34}^2 - 2r_{12}r_{34}\cos(\theta - \theta') + (\alpha)^2\right]^{1.5}} \right] dr_{12}dr_{34}d\theta d\theta'$$

Solving the above equation in MATLAB the value of $F_{y,s}$ was to be 40.0327 N. From the above discussion it can be concluded that the estimated force between two cubical magnets and sector magnets having same surface area was same.

Case study 2: Consider one cuboid magnet with dimensions a=10 mm, c= 20 mm and second cuboid magnet a'=10 mm, c'=20 mm. The dimension of b and b' from 0.01 to 0.1. Consider the magnetic remanence value of both the magnets as 1 T. Let us consider clearance between these magnets is 1 mm. Calculate load carrying capacity between the cuboidal magnets and compare it with load capacity between the equivalent sector magnets for different estimated angular arc of the magnets.

Solution: The dimensions of equivalent sector magnets are found using (R_2-R_1)=a=20 mm, (R_4-R_3)=a'=20, B=c=10 mm, H=c'=10 mm and Clc=1 mm. Assuming R_1=10 mm, R_2= 30 mm, R_3=31 mm and R_4=51 mm. The value of ψ is estimated using equation (11).

The vertical force between two cubical can be estimated using equation (10). Similarly the vertical force between sector magnets can be estimated using equation (12). The forces results are plotted in Fig. 11. From this graph it can be inferred that the value of forces in both cases is almost same till 90^0 and after that the deviation of values starts. Hence from this figure it can be concluded that the equation (11) is valid for $0 > \psi > 90^0$ in this case.
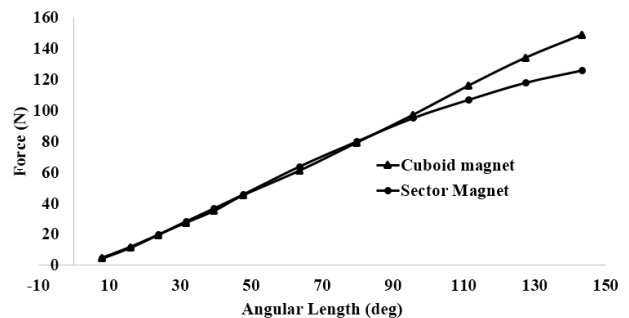

Fig. 11 Comparison of vertical forces between square and sector magnets.

From the above example it can be inferred that the cuboid magnets having same surface area have the same load carrying capacity as sector magnets for same thickness and axial length. Hence equation (12) can be extended for a magnetic bearing having a full ring rotor magnet and stator with 'n' number of cubical magnets, such as:

$$F_{y,s} = \sum_{i=1}^{n} F_{y,s,i} \qquad (13)$$

where:

$$F_{y,s,i} = \frac{\sigma_1 \sigma_2}{4\pi\mu_0} \left(R(z_a, i) + R(z_a + H - B, i) + R(z_a + H, i) + R(z_a - B, i) \right)$$

$$R(\alpha, i) = \int_{\frac{-\Psi}{2}+(i-1)\frac{2\pi}{n}}^{\frac{\Psi}{2}+(i-1)\frac{2\pi}{n}} \int_0^{2\pi} \int_{R_3}^{R_4} \int_{R_1}^{R_2} \left[\frac{\left(e + r_{12}\cos(\theta) - r_{34}\cos(\theta')\right) r_{12} r_{34}}{\left(\begin{array}{c} r_{12}^2 + r_{34}^2 + e^2 - 2r_{12}r_{34}\cos(\theta - \theta') \\ + 2e\left(r_{12}\cos(\theta) - r_{34}\cos(\theta')\right) + (\alpha)^2 \end{array} \right)^{1.5}} \right] dr_{12} dr_{34} d\theta d\theta'$$

Similarly for perpendicular polarization the equation (5) modified for 'n' number of sector magnets and is given by equation (14).

$$F_{y,p} = \sum_{i=1}^{n} F_{y,p,i}$$

$$F_{y,p,i} = A[(z_a, R_1), i] - [A(z_a+h, R_1), i] - [A(z_a, R_2), i] + [A(z_a+h, R_2), i] \qquad (14)$$

where:

$$A\left[(z_a, R_1), i\right] = \int_{\frac{-\Psi}{2}+(i-1)\frac{2\pi}{n}}^{\frac{\Psi}{2}+(i-1)\frac{2\pi}{n}} \int_0^{2\pi} \int_0^L \int_{R_3}^{R_4} \left[\frac{\left(e + R_1\cos(\theta) - r_{34}\cos(\theta')\right)}{\left(\begin{array}{c} R_1^2 + r_{34}^2 + e^2 - 2R_1 r_{34}\cos(\theta - \theta') + \\ 2e\left(R_1\cos(\theta) - r_{34}\cos(\theta')\right) + (z_a - z_{34})^2 \end{array} \right)} \right] dr_{34} dz_{ab} d\theta d\theta,$$

The total radial force by RMD is given by equation (15).

$$F_{y,RMD} = \sum \left(\sum_{j=1}^{k} \sum_{i=1}^{n} F_{y,s,i,j} + \sum_{j=1}^{m} \sum_{i=1}^{n} F_{y,p,i,j} \right) \qquad (15)$$

3. EXPERIMENTAL SETUP DEVELOPMENT

To compare the load carrying capacities of the mentioned two configurations an experimental setup, as shown in Fig. 12, was developed. This experimental setup consists of stainless steel (grade 303) shaft, rotor magnet, aluminium casing, loading arrangement, ball bearing, and rigidly mounted induction motor (AC, 3 phase, 1.5 kW) on a base plate. The stainless steel shaft is connected to motor with a spiral coupling. The loading

arrangement consists of a horizontal loading platform supported on linear bearing mounted on vertical slide ways of circular cross section.
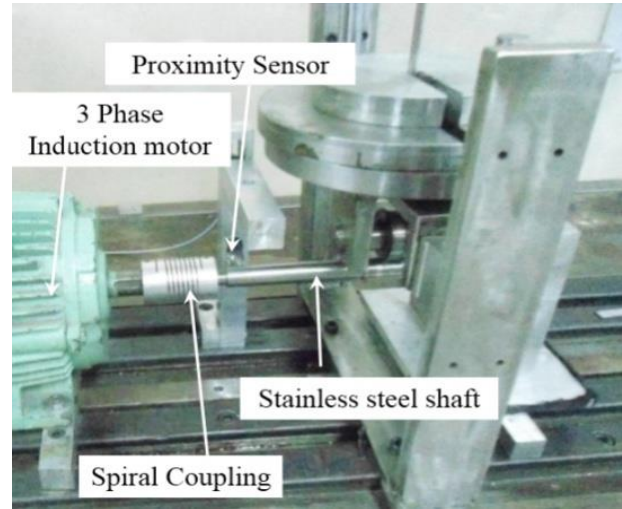
(a) Left side view
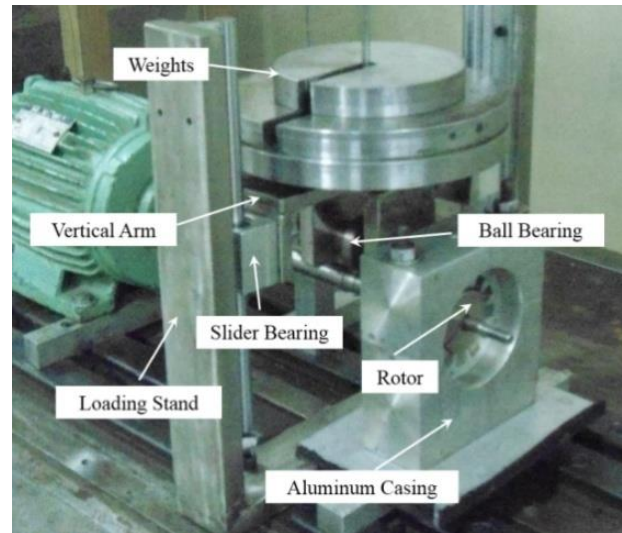
(b) Right side view

Fig. 12. Experimental Setup for magnetic bearing.

A (shielded) deep groove ball bearing transfers the load from the loading platform to the shaft. The displacements of the stainless steel shaft in horizontal and vertical directions were recorded using the proximity sensors and associated proximitors, and (-)24 V DC at sampling frequency of 1kHz. The variation in the voltage was measured using cRio 9202 and voltage module 9201 from National Instruments.

4. RESULTS AND DISCUSSION

In this heading, the results obtained from experimental study have been compared with those of the simulation studies. Two configurations

of bearing (i) Full ring rotor and stator magnets as shown in Fig. (4) and (iii) RMD configuration shown in Fig. (5) were studied.

Configuration 1: In configuration 1 the rotor and the stator magnets are full ring as shown in Figs. 13(a) and 13(b) respectively. The dimension of the magnets considered for calculating the load carrying capacity is given in Table 4. The vertical load carrying capacity for this configuration is estimated by using equation (1). The modified equation for full ring rotor and stator magnet for the present case is given in equation (16).

Table 4. Dimensions of magnets considered for validation.

| Sl. No.	Parameter	
1	Inner radius of rotor (R_1) (mm)	5
2	Outer radius of rotor (R_2) (mm)	24
3	Inner radius of stator (R_3) (mm)	25
4	Outer radius of stator (R_4) (mm)	35
5	Axial length of rotor (B) (mm)	48
6	Axial length of stator (H) (mm)	50
7	Magnetic Remanance value of rotor (T)	0.8
8	Magnetic Remanance value of stator (T)	1.4
9	Axial displacement (z_a) (mm)	0

(a) Rotor

(b) Stator

Fig. 13. Full ring rotor and stator magnet.

$$F_{y,s} = \frac{\sigma_1 \sigma_2}{4\pi\mu_0} \left(R(0) + R(0 + 0.05 - 0.048) + R(z_a + 0.05) + R(z_a - 0.048) \right)$$

(16)

where:

$$R(\alpha) = \int_0^{2\pi} \int_0^{2\pi} \int_{0.025}^{0.035} \int_{0.005}^{0.024} \left[\frac{\left(e + r_{12}\cos(\theta) - r_{34}\cos(\theta') \right) r_{12} r_{34}}{\left(\begin{array}{c} r_{12}^2 + r_{34}^2 + e^2 - 2r_{12}r_{34}\cos(\theta - \theta') \\ + 2e\left(r_{12}\cos(\theta) - r_{34}\cos(\theta') \right) + (\alpha)^2 \end{array} \right)^{1.5}} \right] dr_{12} dr_{34} d\theta d\theta'$$
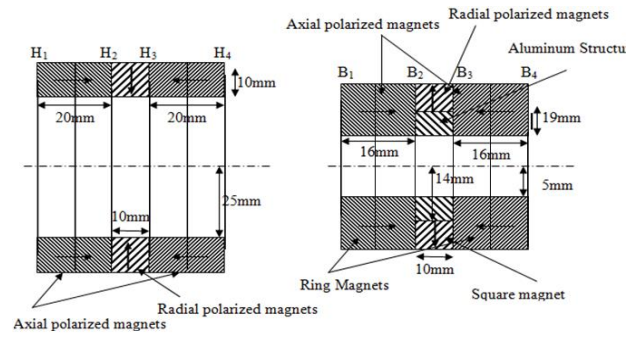
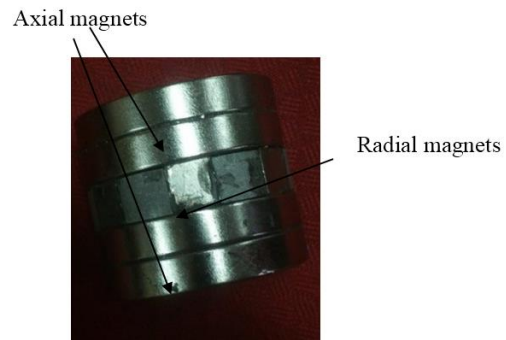| (a) Stator	(b) Rotor

Fig. 14. RMD configuration.

(a) Proposed structure with square magnets

(b) Rotor structure with square magnet

(c) Rotor

Fig. 15. Rotor for RMD configuration.

Configuration 2: The stator and rotor considered for RMD configuration are shown in the Figs. 14 and 15 respectively. Method adopted for developing stator and rotor of this configuration is discussed below.

Development of stator: As depicted in Fig. 15(a), a circular aluminium structure consisting of twelve cuboid slots (in which cuboid magnets will be inserted) was fabricated and attached with another such structure to form a 20 mm long stator. The complete stator is built by attaching two such 20 mm long statorson either side of a radially polarised magnet{shown in Fig. 14(a)}.The stator for RMD arrangement with dimensions is shown in Fig. 14 (a).

Development of rotor: The rotor with radially polarization is developed by fabricating a circular aluminium structure consisting of seven cuboid magnets as shown in Fig. 15(b). Due to the unavailability of 20 mm thick axial polarized magnets, two sets of two ring magnets of 8 mm were attached to form a 16 mm axially polarized magnet. The complete rotor is built by attaching two such 16mm long rotors on either side of a radially polarised magnet {shown in Fig. 14(b)}. The rotor with dimensions considered for RMD configuration is shown in Fig. 15(c). The total load carrying capacity of this configuration was calculated using equation (15).
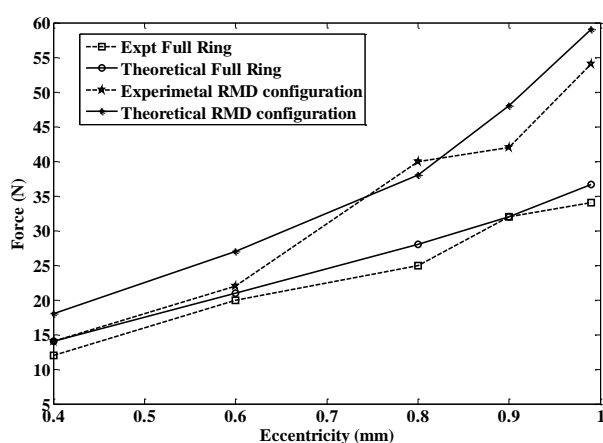

Fig. 16. Theoretical and Experimental comparison of configuration 1 and 2.

The values of vertical force obtained for the configurations 1 and 2 at different eccentricity are plotted presented in Fig. 16. From this figure, it can be concluded that there is close matching in experimental and theoretical results. The load carrying capacity of RMD bearing is

approximately 55 N, while load capacity of full ring bearing is 30 N. It can be concluded that using the proposed RMD structure load carrying capacity can be enhanced by 1.8 time than a full ring axially polarized magnets.

5. CONCLUSION

The theoretical and experimental studies were conducted on the two configurations (configuration 1: full rings axially polarized rotor and stator; and configuration 2: RMD) of passive magnetic bearings. The following are conclusions of this study:

- The sectors magnets do not find wide application due to limitation on their dimensions and inter-changeability of the polarization of the magnets. The cubical magnets can replace the sector magnets.

- The stator and rotor of radial magnetization can easily be made using cubical magnets.

- The load carrying capacity of configuration 2 is 1.8 times higher than that of configuration 1.

Acknowledgment

REFERENCES

[1] S.G. Ghalmea, A. Mankarb and Y.J. Bhaleraoc, 'Effect of Lubricant Viscosity and Surface Roughness on Coefficient of Friction in Rolling Contact', *Tribology in Industry*, vol. 35, no. 4, pp. 330-336, 2013.

[2] H. Hirani, 'Root cause failure analysis of outer ring fracture of four row cylindrical roller bearing', *Tribology Transactions*, vol. 52, no.2, pp. 180-190, 2009.

[3] P.C. Mishraa, 'Analysis of a Rough Elliptic Bore Journal Bearing using Expectancy Model of Roughness Characterization', *Tribology in Industry*, vol. 36, no. 2, pp. 211-219, 2014.

[4] S.J. Patela, G.M. Deheria and J.R. Patela, 'Ferrofluid Lubrication of a Rough Porous Hyperbolic Slider Bearing with Slip Velocity',

Tribology in Industry, vol. 36, no. 3, pp. 259-268, 2014.

[5] H. Hirani, K. Athre and S. Biswas, 'Rapid and Globally Convergent Method for Dynamically Loaded Journal Bearing Design', *Journal of Engineering Tribology*, vol. 212, pp. 207-214, 1998.

[6] H. Hirani, K. Athre and S. Biswas, 'Dynamic Analysis of Engine Bearings', *International Journal of Rotating Machinery*, vol. 5, no.4, pp. 283-293, 1999.

[7] K.P. Lijesh and H. Hirani, 'Development of Analytical Equations for Design and Optimization of Axially Polarized Radial Passive Magnetic Bearing', *ASME, Journal of Tribology*, vol. 137, no. 1, pp. 9, 2015.

[8] K.P. Lijesh and H. Hirani, 'Stiffness and Damping Coefficients for Rubber mounted Hybrid Bearing', *Lubrication Science*, vol. 26, no. 5, pp. 301-314, 2014.

[9] K.P. Lijesh and H. Hirani, 'Design and Development of Halbach Electromagnet for Active Magnetic Bearing', *Progress In Electromagnetics Research C*, vol. 56, pp. 173–181, 2015.

[10] J. Fang, Y. Le, J. Sun and K. Wang, 'Analysis and Design of Passive Magnetic Bearing and Damping System for High-Speed Compressor', *IEEE Transactions on Magnetics*, vol. 48, no. 9, pp. 2528–2537, 2012.

[11] A.V. Filatov and E.H. Maslen, 'Passive Magnetic Bearing for Flywheel Energy Storage Systems', *IEEE transaction on Magnetic*, vol. 37, no. 6, pp. 3913–3924, 2001.

[12] S.C. Mukhopadhyay, T. Ohji and M. Iwahara, 'Modeling and Control of a New Horizontal-Shaft Hybrid-Type Magnetic Bearing', *IEEE transaction on Magnetic*, vol. 47, no.1, pp. 100–108, 2000.

[13] R. Moser, J. Sandtner and H. Bleuler, 'Optimization of Repulsive Passive Magnetic

Bearings', *IEEE Transactions on Magnetics*, vol. 42, no. 8, pp. 2038–2042, 2006.

[14] J.S. Choi and J. Yoo, 'Design of a Halbach Magnet Array Based on Optimization Techniques', *Magnetics, IEEE Transactions on*, vol. 44, no. 10, pp. 2361-2366, 2008.

[15] J.P. Yonnet, 'Passive magnetic bearings with permanent magnets', *Magnetics, IEEE Transactions on*, vol. 14, no. 5, pp. 803-805, 1978.

[16] X. Feipeng, L. Tiecai and L. Yajing, 'A Study on passive magnetic bearing with Halbach magnetized array', in: *International Conference on Electrical Machines and Systems*, pp. 417–420, 2008.

[17] S.M. Muzakkir, K.P. Lijesh and H. Hirani, 'Tribological failure analysis of a heavily-loaded slow speed hybrid journal bearing', *Eng. Fail. Anal.*, vol. 40, pp. 97–113, 2014.

[18] Q. Tan, W. Li and B. Liu, 'Investigations on a permanent magnetic–hydrodynamic hybrid journal bearing', *Tribol. Int.*, vol. 35, no.7, pp. 443–448, 2002.

[19] H. Hirani and P. Samanta, 'Hybrid (hydrodynamic + permanent magnetic) journal bearings', *Proc. Inst. Mech. Eng. Part J J. Eng. Tribol.*, vol. 221, no. 8, pp. 881–891, 2007.

[20] K.P. Lijesh and H. Hirani, Optimization of Eight Pole Radial Active Magnetic Bearing, *ASME, Journal of Tribology*, vol. 137, no. 2, 2015.

[21] G. Akoun, J.P. Yonnet, '3D analytical calculation of the forces exerted between two cuboid magnets', *IEEE transaction on Magnetic*, vol. 20, no. 5, pp. 1962–1964, 1984.

[22] J.P. Yonnet, S. Hemmerlin, E. Rulliere and G. Lemarquand, 'Analytical Calculation of Permanent Magnet Couplings', *IEEE Trans. Magn.*, vol. 29, no. 6, pp. 2932–2934, 1993.